

Irreversible Modification of Red Cell Ca^{2+} Transport by Phenylglyoxal

B. U. RAESS

Department of Pharmacology, Indiana University School of Medicine, Evansville, Indiana 47732

Received March 11, 1993; Accepted May 25, 1993

SUMMARY

Phenylglyoxal, a dicarbonyl modifier of arginyl residues with a high selectivity for anion substrate binding sites in active centers of proteins, was shown to irreversibly modify and inhibit erythrocyte plasma membrane Ca^{2+} transport and $(\text{Ca}^{2+} + \text{Mg}^{2+})$ -ATPase activity. A method that allows the reaction to proceed in the presence of the modifier was used to analyze the kinetics of inactivation. This proved particularly important for the determination of the inactivation rate constant for Ca^{2+} transport, because inside-out vesicles cannot withstand the removal of the inhibitor after preincubation. Analysis of both $(\text{Ca}^{2+} + \text{Mg}^{2+})$ -ATPase and inside-out vesicular Ca^{2+} transport inactivation rate constants using this approach yielded an irreversible inhibition

pattern. This pattern was consistent with the interpretation that both activities underwent noncomplexing nonsaturable reactions with the inhibitor. ATP was shown to compete with phenylglyoxal by reducing its effects on Ca^{2+} transport. Phenylglyoxal did not appear to alter passive permeability of the vesicles to Ca^{2+} and, in concurrently performed vesicular Ca^{2+} uptake and $(\text{Ca}^{2+} + \text{Mg}^{2+})$ -ATPase measurements, exhibited IC_{50} values of 2.9 and 3.4 mM, respectively. These data support the evidence for a functionally essential arginyl residue in the active site of the Ca^{2+} pump/ATPase and provide pharmacological evidence for a tightly coupled ion-motive enzyme complex responsible for Ca^{2+} efflux.

To maintain normal cellular homeostasis, plasma membranes of eukaryotic cells are well regulated, selective, physical barriers that protect cellular components from an environment that is incompatible with intracellular function. A crucial task for these membranes is to participate in establishing and maintaining an ionic intracellular balance that is optimal for cellular performance. Of several cations regulated by this membrane, Ca^{2+} appears to be quite important, because of its ubiquitous and multifaceted role in cellular physiology. In human erythrocytes, a rather low Ca^{2+} concentration of 10^{-7} M is maintained by three major mechanisms, 1) a relatively low passive permeability, 2) the presence of various membranous and cytosolic components that can bind the ion, and 3) an active, primary, Ca^{2+} extrusion pump, without which the erythrocyte would quickly succumb to the consequences of an excessive Ca^{2+} load imposed by electrochemical forces. Most other cells have additional mechanisms to regulate intracellular Ca^{2+} levels, making the erythrocyte an ideal model to selectively study this particular Ca^{2+} ion-motive mechanism. Inferences may then be drawn regarding more complex mammalian cells that have been shown to possess, among other regulatory Ca^{2+} extrusion mechanisms, a Ca^{2+} pump. Often these Ca^{2+} pumps are structurally similar and functionally identical to the one in human erythrocytes.

Over the years several compounds have been shown to interfere with this $(\text{Ca}^{2+} + \text{Mg}^{2+})$ -ATPase/ Ca^{2+} pump, but the identification of specific modification sites and kinetics of inhibition by these drugs has been only slowly forthcoming. Identification of such sites is a desirable goal and, together with a kinetic description, can be helpful in designing high affinity, selective compounds that potentially could be exploited therapeutically.

The present work extends our earlier findings with phenylglyoxal on the irreversible modification of the $(\text{Ca}^{2+} + \text{Mg}^{2+})$ -ATPase (1) and describes the kinetics of Ca^{2+} transport inhibition across inside-out vesicles of erythrocyte membranes. Because of the fragile nature of these vesicular preparations, the kinetics of irreversible inhibition could not be studied using standard methods of exposure and subsequent removal of the inhibitor. These additional manipulations do not interfere with $(\text{Ca}^{2+} + \text{Mg}^{2+})$ -ATPase activity measurements in membrane ghost preparations but resulted in a complete loss of vesicle Ca^{2+} transport activity. However, the application of a technique first described by Tsou and co-workers (2-4) and extended by Gray and Duggleby (5) has allowed for the kinetic analysis of irreversible transport modification in the presence of both substrate and inhibitor. Thus, it is possible to compare and extend observations with phenylglyoxal and the $(\text{Ca}^{2+} + \text{Mg}^{2+})$ -ATPase to primary active vesicular Ca^{2+} transport. The work also provides pharmacological evidence to link $(\text{Ca}^{2+} + \text{Mg}^{2+})$ -

This work was supported in part by a grant-in-aid from the American Heart Association, Indiana Affiliate.

ABBREVIATIONS: $(\text{Ca}^{2+} + \text{Mg}^{2+})$ -ATPase, calcium-activated, magnesium-requiring adenosine 5'-triphosphohydrolase (EC 3.6.1.3); EGTA, ethylene glycol bis(β -aminoethyl ether)-*N,N,N',N'*-tetraacetic acid; HEPES, *N*-2-hydroxyethylpiperazine-*N'*-2-ethanesulfonic acid.

ATPase enzymic activity with the plasma membrane Ca^{2+} transport process.

Experimental Procedures

Materials

Outdated packed human erythrocytes (0–35 days past the expiration date) were generously supplied by the Western Kentucky Regional Blood Bank facility (Owensboro, KY) or Red Cross Blood Services Center (Evansville, IN). Crystalline ATP (disodium salt) was obtained from Boehringer Mannheim (Indianapolis, IN). Phenylglyoxal monohydrate (97%) was purchased from Aldrich Chemicals, Inc. (Milwaukee, WI).

Methods

White ghost membrane preparation. A standard, low ionic strength, hemoglobin-depleting membrane preparation, as typically used for ATPase activity measurements, was prepared according to a procedure described earlier (1).

ATPase assays. Incubation media contained 200 μg of membrane protein, 1 mM ATP, 15 mM KCl, 80 mM NaCl, 0.1 mM EGTA, 3 mM MgCl_2 , 0.2 mM CaCl_2 , 0.1 mM ouabain, 18 mM histamine, and 18 mM imidazole, pH 7.1 at 37° . Freshly prepared phenylglyoxal was added as indicated. The final incubation volume was 1 ml. The reactions were initiated by addition of a concentrated membrane suspension and were incubated in a gently shaking water bath at 37° for up to 90 min. Reactions were terminated by the addition of 1 ml of 2% sodium dodecyl sulfate. An automated colorimetric phosphomolybdate complexation method was used to determine amounts of inorganic phosphate liberated. Complex formation was measured spectrophotometrically at a wavelength of 750 nm (6).

Inside-out vesicle preparations. Packed cells were washed three times in 2 volumes of 154 mM NaCl, containing 0.1 mM EGTA, pH 7.4 at 4° , and the buffy coat was removed by aspiration. The cells were hemolyzed in 40 volumes of 2 mM HEPES buffer, pH 8.1, containing 0.1 mM EGTA, and were centrifuged for 15 min at about $31,000 \times g$ (r_{max}); afterward, the clear supernate and a red pellet were removed. The remaining fluffy fraction was then diluted 1:1 with the hemolyzing buffer and incubated with gentle shaking for 40 min at 37° . The incubation was stopped by placing the membranes on ice for 10 min and then forcefully pushing them four times through a 1-inch-long 25-gauge hypodermic needle. The processed membranes were then washed with 40 volumes of a solution containing 18 mM KCl, 16.5 mM HEPES, 0.1 mM Tris, 0.1 mM EGTA, pH 7.5 at 4° , and were centrifuged for 15 min at $3000 \times g$ (r_{max}). The pooled vesicles were diluted approximately 1:1 in the same solution and stored on ice at an average membrane protein concentration of 3.82 mg/ml. Membrane orientation assessment by acetylcholinesterase accessibility was done by the method of Steck and Kant (7), which yielded an average value of 30.5% inside-out orientation. Membrane protein was estimated by the method of Lowry *et al.* (8), using bovine serum albumin as the standard.

^{45}Ca net uptake into inside-out vesicularized membrane fragments. Basic transport incubation medium (1.0 ml) contained 18 mM imidazole, 18 mM histidine, 15 mM NaCl, 100 mM KCl, 3 mM MgSO_4 , 0.1 mM ouabain, 1 mM ATP, pH 7.1, and 2.0–20 μM CaCl_2 (0.047 mCi/mg). Prewarmed, freshly prepared phenylglyoxal was added to the medium and preincubated for 5 min at 37° . Immediately thereafter, transport was initiated with the addition of 200 $\mu\text{g}/\text{ml}$ membrane protein. At timed intervals of 1–5 min for up to 90 min, 50- μl aliquots were removed from the stirred incubation vessel and diluted into 60 volumes of an ice-cold stopping solution containing 40 mM Tris, 40 mM glycylglycine, 0.1 mM MgCl_2 , and 3 mM CaCl_2 , pH 7.1. The quenched vesicles were trapped on a 0.45- μm , 25-mm-diameter membrane filter (Metrical GA-6; Gelman) under 15 psi negative pressure. The filters were immersed in a complete counting cocktail (RPI 3a70B) and measured in a Beckman LS 7500 scintillation counter.

Data analysis. Curve fitting of the data was done by least square

polynomial regression analysis, and extrapolated values for $[P]_\infty$ (the product concentration at time infinity) were obtained by a trend analysis procedure, fitting a curve based on the function $Z = \exp(a + b/t)$. Coefficients were obtained by least squares fitting after taking the natural logarithm of Z . In figures representing averages from three experiments, error bars on curves represent standard errors and, where absent, indicate a value smaller than the symbol size.

Results

Initial (0–3 min) transport rates of net Ca^{2+} uptake into control and phenylglyoxal-exposed inside-out red blood cell vesicles are depicted in Fig. 1. Vesicles were incubated in the presence of 20 μM Ca^{2+} for 60 min at 37° , with phenylglyoxal concentrations ranging from 0.3 to 3 mM. Phenylglyoxal in these vesicles could not be removed by standard washing procedures. Control vesicle preparations in which phenylglyoxal removal was attempted lost all Ca^{2+} transport capabilities. Therefore, to indicate the irreversible nature of phenylglyoxal and to minimize its effects during the actual uptake measurements, phenylglyoxal was diluted 20-fold to concentrations that are not likely to contribute significantly to the inhibition. In three separate preliminary experiments, basal, i.e., calmodulin-independent, rates of uptake (shown as raw counts of Ca^{2+} net uptake) were linear with time and were inhibited by phenylglyoxal in a concentration-dependent manner. Inhibition by 3 mM phenylglyoxal after 60 min was nearly complete ($96.3 \pm 0.3\%$) and exhibited a concentration-effect relationship with an apparent IC_{50} of 0.771 mM phenylglyoxal (Fig. 1, inset). Data points on the ordinate represent “zero-time” samples (aliquots removed immediately upon mixing of incubation com-

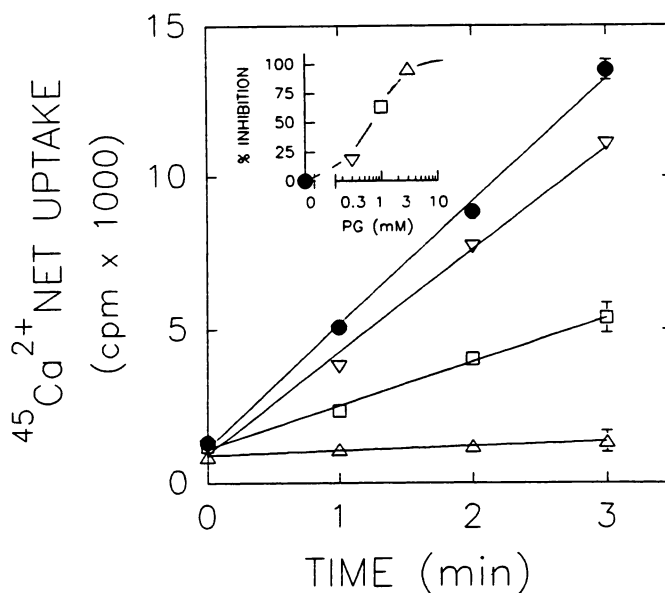


Fig. 1. Inhibition of short term vesicular $^{45}\text{Ca}^{2+}$ net uptake after preexposure to and incubation in the presence of phenylglyoxal. Inside-out vesicles (4 mg/ml) were incubated for 60 min at 37° in the presence of 0 (\bullet), 0.3 mM (∇), 1.0 mM (\square), or 3.0 mM (\triangle) phenylglyoxal. After exposure, aliquots of membrane and phenylglyoxal were transferred into transport incubation medium and assessed for Ca^{2+} uptake activity. Final membrane concentrations during transport were 200 $\mu\text{g}/\text{ml}$, ATP concentration was 1.0 mM, and phenylglyoxal concentration was 0, 15, 50, or 150 μM . Inset, semilogarithmic plot of the inhibition (percentage of control) as a function of phenylglyoxal concentrations during the 60-min preincubation period. Data represent the means of three independent experiments. Error bars, standard errors.

ponents) and are assumed to represent nonspecific binding of the isotope to membranes and filters. The rate of passive leakage into vesicles in the absence of exogenously added ATP and phenylglyoxal was negligible ($<0.2\%$ of control after 60 min) (data not shown).

Fig. 2 shows $(\text{Ca}^{2+} + \text{Mg}^{2+})$ -ATPase activities both in the absence and in the presence of 1–3 mM phenylglyoxal in a white ghost preparation. Enzyme activity under control conditions in the absence of the inhibitor was linear over a 90-min time period. Although in this type of preparation effective removal of inhibitor and thus termination of the phenylglyoxalation is possible (1), data shown in Fig. 2 represent experiments in which the enzyme was exposed to phenylglyoxal throughout the ATPase assay incubation period. This set of experiments was included to compare kinetic parameters determined by using the Tsou analysis in the present transport studies with previously determined kinetic values and observations from this laboratory. Maximal product formation at infinite time for the three phenylglyoxal concentrations, P_{∞} , was estimated using a trend analysis forecasting procedure based on a least square fitted curve [using the function $Z = \exp(a + b/t)$]. P_{∞} values thus estimated were 127, 52, and 32 nmol of $\text{P}_i/100 \mu\text{g}$ of membrane protein for the curves in the presence of 1, 2, and 3 mM phenylglyoxal, respectively. Fig. 2, *inset*, shows an excerpt of the first 45 min plotted semilogarithmically for the three phenylglyoxal concentrations. Pseudo-first-order inactivation curves are observed, from which the apparent rate of inactivation can be calculated using the equation $[P] = \ln[P]_{\infty} - A[Y]t$, where $[P]_{\infty}$ is the product concentration at infinite time, A is the inactivation rate constant, and Y is the inhibitor. At time infinity $[P]_{\infty}$ becomes a constant value, which decreases as the inhibitor concentration ($[Y]$) increases, and plots of $\ln[P]_{\infty} - [P]$ versus time yield straight lines with slopes of $-A[Y]$. Accordingly, from these slopes (Fig. 2, *inset*) an apparent rate constant of inactivation of $0.01024 \pm 0.00019 \text{ min}^{-1}$ for phenylglyoxal on white ghost $(\text{Ca}^{2+} + \text{Mg}^{2+})$ -ATPase activity in the presence of 1 mM ATP was obtained.

To establish nonsaturation kinetics and to differentiate between complexing and noncomplexing irreversible reactions, data shown in Fig. 2 were replotted in double-reciprocal plots

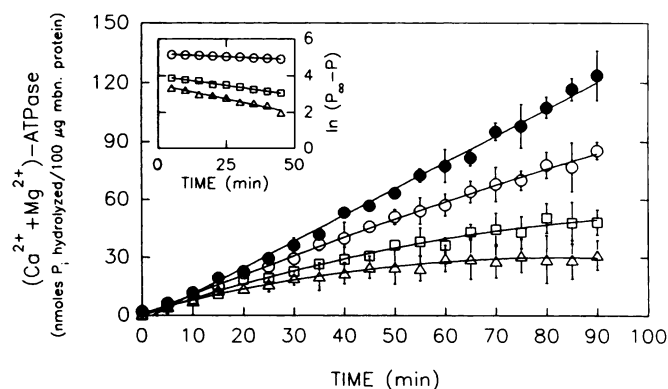


Fig. 2. $(\text{Ca}^{2+} + \text{Mg}^{2+})$ -ATPase inactivation by exposure to phenylglyoxal. Long term concomitant exposure to 0 mM (●), 1 mM (○), 2 mM (□), or 3 mM (Δ) phenylglyoxal and enzymic activity assessment in a white ghost membrane preparation. Substrate, 1.0 mM ATP. *Inset*, semilogarithmic plot of apparent rates of inactivation. Curves were fitted by linear regression [*inset* and control (●)] or by polynomial fitting of the second order. Data are from two membrane preparations and four independent experiments measured in duplicate. Error bars, standard errors.

(Fig. 3). Fig. 3A depicts the reciprocal of the observed inactivation rate constant as a function of the inverse phenylglyoxal concentration. This yields an extrapolated line through the points that intercepts the origin of the plot, which is indicative of nonsaturation kinetics, i.e., a direct proportionality of the inactivation process to the inhibitor concentration. Wang *et al.* (4) have shown that the expression for the apparent rate constant of complexing reactions is different from that of noncomplexing reactions, in that it contains the term for the inhibitor concentration. However, for noncomplexing reactions ($E + Y \rightarrow EY$), the rate constant is independent of inhibitor concentration and yields a line parallel to the abscissa when plotted against the inhibitor concentration, as shown in Fig. 3B.

Fig. 4 shows an analogous transport experiment that demonstrates the effects of phenylglyoxal on the long term net uptake of $^{45}\text{Ca}^{2+}$ into inside-out erythrocyte vesicles, using 1.0 mM ATP and $2.0 \mu\text{M}$ Ca^{2+} in the incubation medium. Unlike the $(\text{Ca}^{2+} + \text{Mg}^{2+})$ -ATPase reaction, which remains linear over a 90-min period, Ca^{2+} net uptake after 20–30 min starts to deviate from linearity and eventually reaches a plateau, where rates of uptake equal passive efflux of Ca^{2+} from the vesicular lumen. Phenylglyoxal (1–3 mM) decreases both initial rates of uptake and the level to which Ca^{2+} is able to accumulate, in a

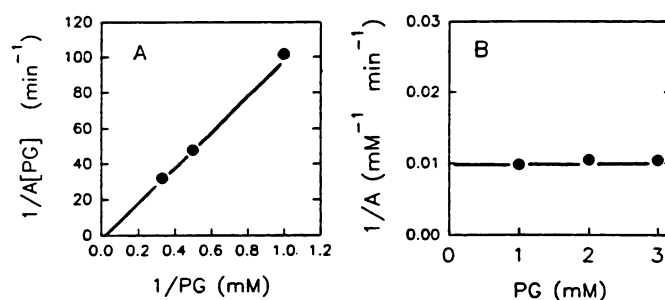


Fig. 3. Determination of nonsaturation noncomplexing reaction kinetics. A, Double-reciprocal plot of the observed inactivation constant (k_{obs}) $1/A[PG]$ versus phenylglyoxal (PG) concentration. A was calculated from the slopes of the plots in Fig. 2 (*inset*), which correspond to $-A[PG]$, based on the equation $\ln(P_{\infty} - P) = \ln(P_{\infty}) - A[PG]t$ (4). The second-order rate constant in the presence of 1.0 mM ATP is 0.175 sec^{-1} . B, Plot of the reciprocal constant of inactivation for a noncomplexing reaction, $E + Y \rightarrow EY$.

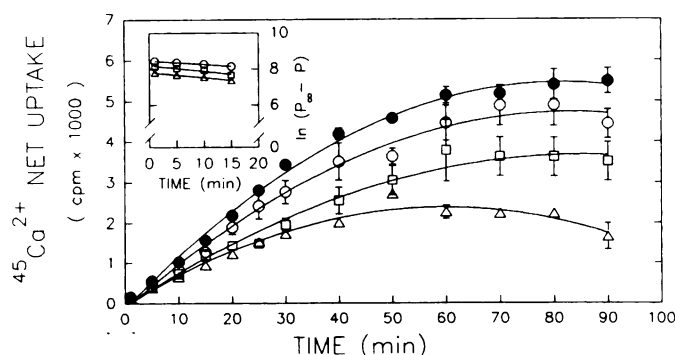


Fig. 4. $^{45}\text{Ca}^{2+}$ net uptake into inside-out vesicles. Inhibition in the presence of phenylglyoxal. Transport experiments analogous to $(\text{Ca}^{2+} + \text{Mg}^{2+})$ -ATPase measurements shown in Fig. 2. ●, 0 mM; ○, 1.0 mM; □, 2.0 mM; Δ, 3.0 mM phenylglyoxal. Data are means and standard errors of three independent experiments. All curves were fitted with linear (*inset*) or polynomial regressions of the second degree. *Inset*, semilogarithmic plot of apparent rates of inactivation fitted by linear regression analysis.

concentration-dependent manner. Fig. 4, *inset*, depicts the initial linear 15-min portion of uptake plotted in a semilogarithmic transformation of activity remaining in the presence of the three phenylglyoxal concentrations. Again, a pseudo-first-order inactivation, from which the apparent rate of transport inactivation can be calculated, is shown. The same trend analysis procedure to estimate $[P]_{\infty}$ as used in Fig. 2 was used and yielded an apparent rate constant of inactivation of $0.01368 \pm 0.00297 \text{ min}^{-1}$ for phenylglyoxal in the presence of 1 mM ATP.

The rate of net $^{45}\text{Ca}^{2+}$ uptake starts to diminish after 20–30 min and reaches a plateau around 60 min. In the presence of phenylglyoxal, this plateau is diminished in a concentration-dependent manner, which reflects the uptake capacity in the presence of a constant passive permeability that apparently is not affected by phenylglyoxal itself. With 3 mM phenylglyoxal, the steady state between 60 and 90 min was decreased to roughly 44% of control values, indicating a complete cessation of net uptake activity. The lack of phenylglyoxal effects on passive Ca^{2+} fluxes was corroborated by an independent set of experiments in which the vesicles were exposed to phenylglyoxal (0.5 mM, 2 mM, and 10 mM for 30 min; two experiments) in the absence of ATP. No change in passive permeability or "tightness" of the vesicle preparation, i.e., no observable net uptake, was seen at any phenylglyoxal concentration (Fig. 5).

Active site protection from covalent phenylglyoxal modification by the ATP substrate is demonstrated in Table 1. When the ATP concentration was increased from 0.5 mM to 1.0 mM or 2.0 mM, inactivation by 1 mM phenylglyoxal was reduced from 39% to 20% and 19%, respectively.

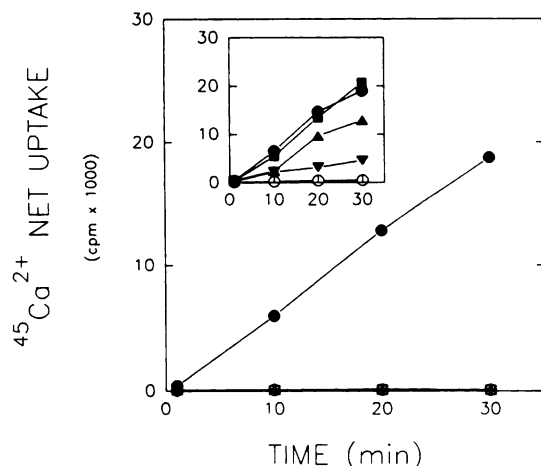


Fig. 5. Lack of phenylglyoxal effects on apparent passive $^{45}\text{Ca}^{2+}$ permeability properties of inside-out vesicles. Effects of 0.5 (\square), 2.0 (Δ), and 10 (∇) mM phenylglyoxal in the absence of ATP; \bullet , control, 1 mM ATP, no phenylglyoxal (two experiments). *Inset*, 0 (control) (\bullet), 0.5 (\blacksquare), 2.0 (\blacktriangle), and 10 (\blacktriangledown) mM phenylglyoxal in the presence of 1.0 mM ATP; \circ , no ATP, no phenylglyoxal (one experiment). Same axis labels apply.

TABLE 1

Effects of ATP on Ca^{2+} transport inactivation by 1 mM phenylglyoxal

[ATP] mM	n*	Transport inhibition	
		1 min	30 min
		%	
0.5	3	<1	39
1.0	3	4	20
2.0	2	0	19

* n, number of experiments.

Fig. 6 shows concomitant $(\text{Ca}^{2+} + \text{Mg}^{2+})$ -ATPase and Ca^{2+} transport experiments in which the same inside-out vesicular preparation was used after exposure to 0.2–10 mM phenylglyoxal. Fig. 6 shows a good degree of concordance in plots of residual $(\text{Ca}^{2+} + \text{Mg}^{2+})$ -ATPase and Ca^{2+} transport activities from two different preparations after a 30-min incubation in the presence of various concentrations of phenylglyoxal. The average specific activity for the unmodified $(\text{Ca}^{2+} + \text{Mg}^{2+})$ -ATPase activity (100%) was $7.17 \pm 1.24 \text{ nmol of } \text{P}_i \text{ hydrolyzed/mg of membrane protein/min}$ (mean \pm standard error, three experiments) and for unmodified Ca^{2+} transport (100%) was $0.250 \pm 0.093 \text{ nmol of } \text{Ca}^{2+} \text{ transported/mg of membrane protein/min}$ (mean \pm standard error, three experiments), corrected for the degree of sidedness in each of the preparations. Under these experimental conditions [1 mM ATP/20 μM Ca^{2+} (ATPase) and 1 mM ATP/2 μM Ca^{2+} (transport), 30-min exposure at 37°], IC_{50} values of about 3 mM phenylglyoxal were obtained for the transport and ATPase activities.

Discussion

Because of the ubiquitous role of Ca^{2+} as a primary and secondary messenger in cellular function, it is important to understand its intracellular regulation. For this, the red cell plasma membrane has served a useful role in delineating the biochemical, biophysical, and pharmacological aspects of the $(\text{Ca}^{2+} + \text{Mg}^{2+})$ -ATPase and Ca^{2+} transport mechanism. However, unlike the situation with the Na^{+} - K^{+} pump and its highly specific inhibitor ouabain, an analogously useful, specific, and selective antagonist that links enzymic and transport activities for the Ca^{2+} pump has remained elusive. In an attempt to fill this void we have embarked on the classification and description of several compounds that have been reported to interfere with this particular pump mechanism by a variety of different means, including covalent modification of the protein by phenylglyoxal (9).

Irreversible modifications of arginine side chains by simple

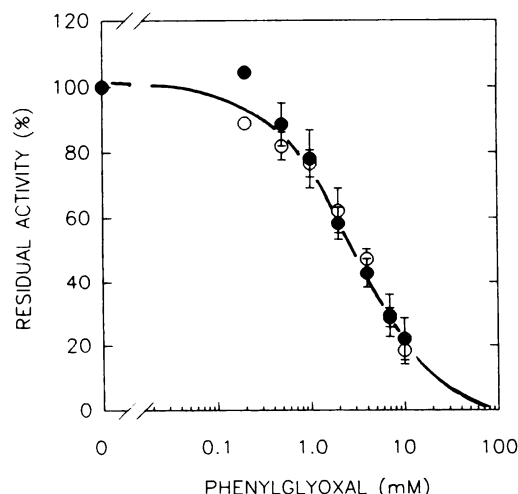
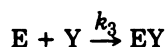


Fig. 6. Phenylglyoxal inhibition of concurrent $(\text{Ca}^{2+} + \text{Mg}^{2+})$ -ATPase and $^{45}\text{Ca}^{2+}$ net uptake in inside-out vesicles. Dose-response curves of phenylglyoxal for concurrently assessed enzyme (\circ) and transport (\bullet) activities in the same vesicular preparations. Results are plotted as percentage of normalized residual activity remaining after 30-min exposure to phenylglyoxal concentrations of 0.2–10.0 mM in the presence of 1.0 mM ATP. Data are the means of two (0.2 mM phenylglyoxal) or three independent experiments. Error bars, standard errors.

α -dicarbonyl compounds, such as phenylglyoxal, are well known for their selectivity for this amino acid (10–14). This is coupled with a particular susceptibility of arginyl residues at enzymic anion recognition sites and/or active centers with anionic substrates (12, 13). Because our original description of phenylglyoxal effects on the Ca²⁺ pump was limited to (Ca²⁺+Mg²⁺)-ATPase measurements (1), the irreversibility of phenylglyoxal modification of Ca²⁺ transport (15) (Fig. 1) was only presumptive. The reason for this is that the inside-out vesicle preparation is too fragile to withstand the manipulations associated with the physical removal of phenylglyoxal from the incubation medium. Therefore, to compare and link the effects of phenylglyoxal on ATPase activity with those on Ca²⁺ transport, the present work applies an approach first described by Tsou and co-workers (2–4) and modified by Gray and Duggleby (5). This method allows for the kinetic analysis of covalent enzyme modifications by measuring substrate reactions in the presence of the modifier. Considering the experimental route chosen, the values presented here for P_{∞} -derived rates of inactivation in the presence of inhibitor and 1 mM ATP for this type of preparation (i.e., 0.1706 M⁻¹ sec⁻¹ for the enzymic activity and 0.2281 M⁻¹ sec⁻¹ for transport) compare quite favorably with previously published rates of ATPase inactivation of 0.173–0.620 M⁻¹ sec⁻¹. The latter values were obtained from experiments on white ghost erythrocyte membranes in the presence of 0–6 mM ATP. This involved preincubating the membranes with phenylglyoxal, followed by the removal of the inhibitor and enzyme activity assessment (1).

Another confirmation of the validity of applying the P_{∞} method to this question is that this analysis also yielded non-saturation kinetics, with a comparable second-order rate constant of 0.175 sec⁻¹ in the presence of 1 mM ATP (Fig. 3A) and a plot parallel to the abscissa when the reciprocal rate constant of inactivation was plotted against the inhibitor concentration, which is indicative of a noncomplexing reaction. This also corroborates our initial proposals for the inactivation of the (Ca²⁺+Mg²⁺)-ATPase enzymic activity by standard preincubation-inhibitor removal procedures (1) and indeed suggests a modification mechanism that fits the expression



An added dividend from the long term (Ca²⁺+Mg²⁺)-ATPase measurements of P_{∞} was the demonstration of the known, but rarely confirmed, remarkable stability and linearity of the ATPase reaction under nearly optimal V_{\max} conditions, i.e., 2×10^{-6} M free Ca²⁺, 1 mM ATP, and 37°. After 90 min under control conditions (no phenylglyoxal present), >87% of the initial substrate concentration remained, which represents a value that is well above the two (low and high) K_m values of 3.5 and 120 μ M, respectively (16). This situation, however, does not apply to the analogous Ca²⁺ transport measurements. In fact, because of the small vesicular volume, high concentrations of Ca²⁺ are reached rather quickly, which necessitates performing the transport experiments at a suboptimal 2 μ M Ca²⁺ concentration to obtain reasonably linear initial uptake rates (up to about 15–20 min). Even with this relatively low Ca²⁺ concentration, ⁴⁵Ca²⁺ net uptake measurements beyond 20 min are curvilinear in nature. This is accounted for by an increasing passive efflux once the intravesicular Ca²⁺ concentration starts to approach an estimated maximum of 2.3 mmol (17). To examine whether the observed phenylglyoxal effects were in-

deed on the active Ca²⁺ transport itself and not the result of a passive permeability change of the vesicular membrane, the effects of phenylglyoxal (up to 10 mM) on the passive “reversed efflux” permeability properties of the vesicles were examined. To check this, the substrate ATP was simply omitted from the incubation medium. Although no Ca²⁺ chelator was incorporated into the vesicles, a decrease in vesicle tightness or increased “inward leak,” as one would expect with the addition of a Ca²⁺ ionophore (17), was not observed (Fig. 5). This can be used to support the argument that phenylglyoxal does not promote increased passive permeability and that the decrease in P_{∞} is indeed a reflection of active pump inhibition. Direct measurements of phenylglyoxal effects on passive Ca²⁺ fluxes are currently underway in this laboratory.

The demonstration of the appropriateness of determining kinetic parameters in the presence of phenylglyoxal allowed us to determine the apparent IC₅₀ for phenylglyoxal by assessing the concentration-effect relationships of the inhibitor for both the Ca²⁺ transport and the (Ca²⁺+Mg²⁺)-ATPase activity, simultaneously and in the same preparation. From computer-fitted curves, virtually identical half-maximally inhibitory concentrations of 2.89 mM and 3.37 mM phenylglyoxal were obtained. These values, derived from experiments run over a 30-min incubation period, are almost 3 times higher than those for the experiment shown in Fig. 1. Aside from the longer incubation period, no obvious explanation for the remaining small difference can be offered, other than the fact that the transport times were 3 versus 30 min in the two experiments. It is possible that small but cumulatively significant differences in the degree of phenylglyoxal hydration, the positive electrostatic potential of the guanidino group on the reactive arginine, or the degree of ionization of a monocarbinolamine intermediate other than the essential arginine in the active center are generated as a consequence of prolonged incubation times. Although presumably controlled for, small changes in these parameters, as well as the type of buffer, pH of the incubation medium, and nucleophilicity of the primary amines present in the buffer, are known to contribute considerably to the degree of the phenylglyoxylation reaction (12–14).

The roughly 30-fold difference in specific rates of 7.17 nmol/mg/min and 0.25 nmol/mg/min for the enzymic and transport activities, respectively, is explained and can be accounted for by the different Ca²⁺ concentrations used. For this reason, the difference in values should not be interpreted as an indication of altered stoichiometry of the pump. In fact, the good concordance of the shapes of the two curves suggests that phenylglyoxal does not change the Ca²⁺/ATP ratio or the ratio of work to energy expenditure for the enzyme-pump complex.

In summary, the present work validates a new approach to characterize kinetically the phenylglyoxal inhibition of plasma membrane Ca²⁺ transport and (Ca²⁺+Mg²⁺)-ATPase, in the presence of the modifying agent. This has made it possible to study the effects of phenylglyoxal (and potentially other irreversible inhibitors) on the Ca²⁺ transport process itself by using inside-out red cell vesicles. Together with our previous findings (1), the data presented here lend further support for a mechanism of action of phenylglyoxal on the Ca²⁺ pump involving the irreversible modification of one arginyl residue at the active center that can be protected by ATP. Moreover, measuring the inactivation process in the presence of phenylglyoxal also supports our earlier findings that indicate nonsaturation kinetics

of the modification without the formation of a measurable intermediary complex. Finally, the high degree of concordance of the various kinetic parameters measured is another example of the use of a drug as a tool to pharmacologically link the enzymic ($\text{Ca}^{2+} + \text{Mg}^{2+}$)-ATPase activity to the biophysical Ca^{2+} transport phenomenon across the plasma membrane.

Acknowledgments

I am grateful for the dedicated expert technical assistance of Donna Record and I thank Dr. G. Tunncliffe for his helpful advice throughout this project. The generous supply of outdated packed red cells by the local blood banks is also gratefully acknowledged.

References

1. Raess, B. U., D. M. Record, and G. Tunncliffe. Interaction of phenylglyoxal with the human erythrocyte ($\text{Ca}^{2+} + \text{Mg}^{2+}$)-ATPase: evidence for the presence of an essential arginyl residue. *Mol. Pharmacol.* 27:444-450 (1985).
2. Tian, W.-X., and C.-L. Tsou. Determination of the rate constant of enzyme modification by measuring the substrate reaction in the presence of the modifier. *Biochemistry* 21:1028-1032 (1982).
3. Liu, W., and C.-L. Tsou. Determination of rate constants for the irreversible inhibition of acetylcholine esterase by continuously monitoring the substrate reaction in the presence of the inhibitor. *Biochim. Biophys. Acta* 870:185-190 (1986).
4. Wang, Z.-X., B. Preiss, and C.-L. Tsou. Kinetics of inactivation of creatine kinase during modification of its thiol groups. *Biochemistry* 27:5095-5100 (1988).
5. Gray, P. J., and R. G. Duggleby. Analysis of kinetic data for irreversible enzyme inhibition. *Biochem. J.* 257:419-424 (1989).
6. Raess, B. U., and F. F. Vincenzi. A semi-automated method for determination of multiple membrane ATPase activities. *J. Pharmacol. Methods* 4:273-283 (1980).
7. Steck, T. L., and J. A. Kant. Preparation of impermeable ghosts and inside-out vesicles from human erythrocyte membranes. *Methods Enzymol.* 31:172-180 (1974).
8. Lowry, O. H., N. J. Rosebrough, A. L. Farr, and R. J. Randall. Protein measurement with the Folin phenol reagent. *J. Biol. Chem.* 193:265-275 (1951).
9. Raess, B. U. Pharmacological modification of the red cell Ca^{2+} -pump, in *The Red Cell Membrane* (B. U. Raess and G. Tunncliffe, eds.). The Humana Press, Inc., Clifton, NJ, 305-327 (1989).
10. Takahashi, K. The reaction of phenylglyoxal with arginine residues in proteins. *J. Biol. Chem.* 243:6171-6179 (1968).
11. Bjerrum, P. J., J. O. Wieth, and C. L. Borders, Jr. Selective phenylglyoxalation of functionally essential arginyl residues in the erythrocyte anion transport protein. *J. Gen. Physiol.* 81:453-483 (1983).
12. Riordan, J. F., K. D. McElvany, and C. L. Borders, Jr. Arginyl residues: anion recognition sites in enzymes. *Science (Washington D. C.)* 195:884-886 (1977).
13. Patthy, L., and J. Thesz. Origin of the selectivity of α -dicarbonyl reagents for arginyl residues of anion-binding sites. *Eur. J. Biochem.* 105:387-393 (1980).
14. Baburaj, K., and S. Durani. Exploring arylglyoxals as the arginine reactivity probes: a mechanistic investigation using the buffer and substituent effects. *Bioorg. Chem.* 19:229-244 (1991).
15. Raess, B. U. Inhibition of human erythrocyte ($\text{Ca}^{2+} + \text{Mg}^{2+}$)-ATPase and Ca^{2+} -transport by phenylglyoxal. *Fed. Proc.* 44:5 (1985).
16. Stieger, J., and S. Luterbacher. Some properties of the purified ($\text{Ca}^{2+} + \text{Mg}^{2+}$)-ATPase from human red cell membranes. *Biochim. Biophys. Acta* 641:270-275 (1981).
17. Hinds, T. R., B. U. Raess, and F. F. Vincenzi. Plasma membrane Ca^{2+} transport: antagonism by several potential inhibitors. *J. Membr. Biol.* 58:57-65 (1981).

Send reprint requests to: B. U. Raess, Department of Pharmacology, Indiana University School of Medicine, P.O. Box 3287, Evansville, IN 47732.
